# THE MM5 NUMERICAL MODEL TO CORRECT PSINSAR ATMOSPHERIC PHASE SCREEN

**D. Perissin[(1)], E. Pichelli[(2)], R. Ferretti[(2)], F. Rocca[(3)] and N. Pierdicca[(4)]**

*[(1)] ISEIS, CUHK, Shatin, NT, Hong Kong, Email: daniele.perissin@cuhk.edu.com*
*[(2)] CETEMPS, Università de L'Aquila, Italy*
*[(3)] DEI, POLIMI, Milano, Italy*
*[(4)] DIE, La Sapienza, Roma, Italy*

## ABSTRACT

In this work we make an experimental analysis to research the capability of Numerical Weather Prediction (NWP) models as MM5 to produce high resolution (1km-500m) maps of Integrated Water Vapour (IWV) in the atmosphere to mitigate the well-known disturbances that affect the radar signal while travelling from the sensor to the ground and back. Experiments have been conducted over the area surrounding Rome using ERS data acquired during the three days phase in '94 and using Envisat data acquired in recent years. By means of the PS technique SAR data have been processed and the Atmospheric Phase Screen (APS) of Slave images with respect to a reference Master have been extracted. MM5 IWV maps have a much lower resolution than PSInSAR APS's: the turbulent term of the atmospheric vapour field cannot be well resolved by MM5, at least with the low resolution ECMWF inputs. However, the vapour distribution term that depends on the local topography has been found quite in accordance.

## 1. INTRODUCTION

Water vapor is one of the most significant constituents of the atmosphere because its phase changes are responsible for clouds and precipitation, whose interaction with electromagnetic radiation is a crucial factor in atmospheric system regulation. Despite of its importance within atmospheric processes over a wide range of spatial and temporal scales, water vapor is one of the least understood and poorly described components of the atmosphere.

Current Numerical Weather Prediction (NWP) models can provide high spatial resolution able to reproduce realistic vapor distribution fields, but one of their most limiting factors is the poor resolution of the initial condition. On the other hand, from the point of view of SAR interferometric applications (e.g., earth motion monitoring), one of the biggest sources of noise for InSAR techniques is the delay caused by changes in the distribution of water vapor in the atmosphere [1]. By analyzing single interferograms, the water vapor delay contribution is practically indistinguishable from ground motion signal with amplitudes that can range from some millimeters up to several centimeters or even greater, leading to a real difficulty to detect ground deformations events. Several efforts have been spent to solve this problem [2], by developing methods to mitigate water vapor artifacts by reconstructing the most likely atmospheric scenario. Most known techniques tend to use observations, such as radiosondes, GPS receiver networks, ground or space based radiometers: the latter generally exhibit poor temporal or spatial resolution, and their accuracy may strongly depend on the surface (land/water) background over which the measurements are acquired [2]. Water vapor field, produced by NWP, can provide a good support to eliminate some of these problems. Meteorological model simulations, indeed, can be used to predict atmospheric delay to be subtracted from InSAR interferograms and to reduce noise on the geodetic signal.

In this paper, the preliminary results of high resolution water vapor field analysis are presented. The MM5 model version 3 [3] is used to produce high resolution water vapor fields to be compared with InSAR data, which have been processed with the Permanent Scatterers (PS) technique [4].

## 2. TECHNICAL FRAMEWORK

In order to compare SAR atmospheric phase screen (APS) and MM5 water vapor maps, some considerations have to be made.

- The two maps are required to be geocoded on the same grid in geographical coordinates. The MM5 grid has been taken as reference and the APS maps have been interpolated on it.
- The APS collects all spatially correlated noise in an interferogram. This means that also residual orbital errors can be included in APS maps. To get rid of such phase trends that can invalidate the comparison, a phase ramp has to be estimated in each interferogram and removed.
- To compare the two quantities, the electromagnetic delay has to be converted into height of integrated water vapor, by means of the well known formula [5] $$ZWD \approx 6.4IWV \qquad (1)$$
- By considering that the water vapor map integrates along the vertical direction while the radar is looking with an incidence angle of approximately 23°, the cosine of the angle has to be accounted for

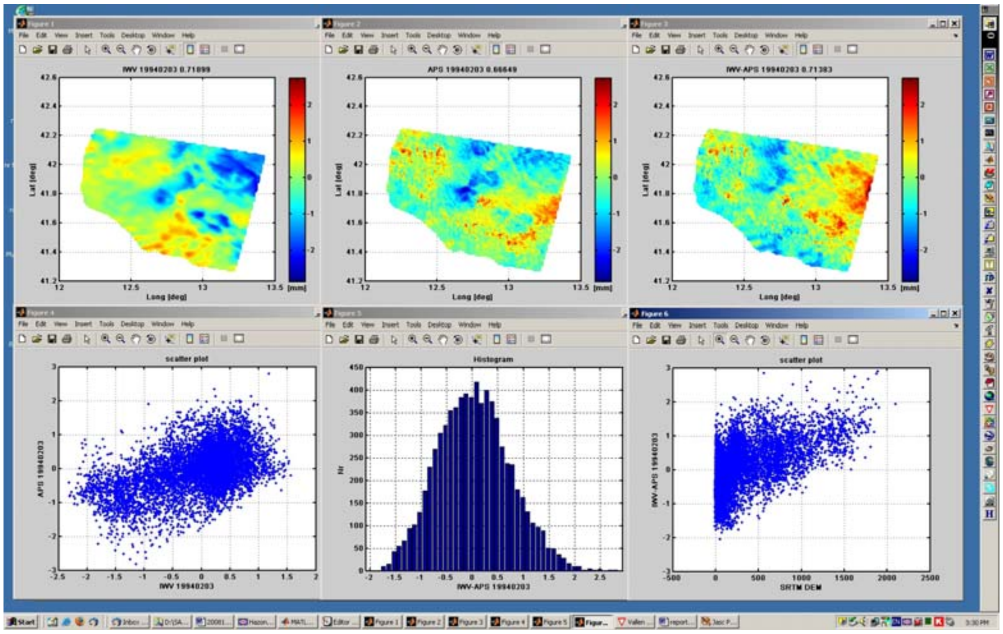

**Figure 1.** Comparison between MM5 and InSAR IWV maps example using ERS1 data acquired in '94 during the 3 days phase. From left to right, starting from the first raw: MM5 IWV map, InSAR map, difference MM5-InSAR, scatter-plot between InSAR and MM5, histogram of differences, residuals as a function of the terrain height.

to map the water vapor in the satellite line of sight.

- InSAR data is a differential measure: each estimated APS is the difference of water vapor delays in two different dates. All available APS's have been referred to a common date (as it is implemented in the classical PS processing chain [4]). In this way, all APS's are affected by a common trend deriving by the reference image. Simply by averaging all available APS's together, the delay map of the reference image can be estimated and removed.
- The tropospheric delay can be modeled as a function of two main terms: a turbulent term and a quantity proportional to the terrain height [6]

$$\alpha_i = \varepsilon_i + k_i q \qquad (2)$$

where $\alpha_i$ is the tropospheric delay, $\varepsilon_i$ the turbulent term, $q$ the terrain height and $k_i$ a proportionality constant.

The proportionality constant changes depending on the local atmospheric parameters (humidity, pressure and temperature) [7], but in any case the tropospheric delay decreases with the height. Thus we can write

$$k_i = k_0 + \delta k_i \qquad (3)$$

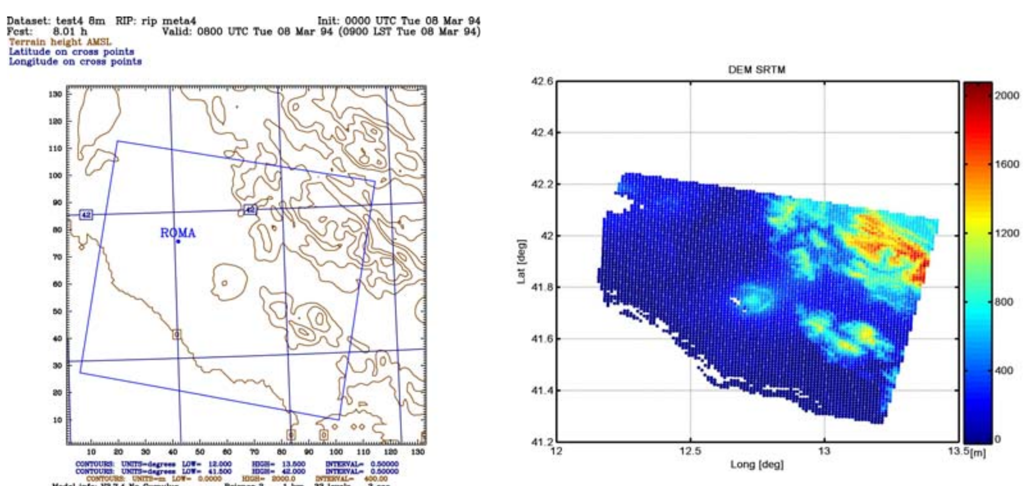


**Figure 2.** MM5 domain (left) and corresponding Digital Elevation Model (right) over the analyzed area in Rome.

| | Nov-02 | Dec-02 | Aug-03 | Dec-03 | Jan-04 | Apr-04 | May-04 | Aug-04 | Oct-04 | Jan-05 |
|---|---|---|---|---|---|---|---|---|---|---|
| InSAR | 0.51 | 0.49 | 1.08 | 0.54 | 0.87 | 0.76 | 0.59 | 0.96 | 0.92 | 1.08 |
| MM5 | 0.43 | 0.60 | 1.26 | 0.44 | 0.97 | 0.28 | 0.46 | 1.34 | 0.95 | 0.84 |
| | Jul-05 | Aug-05 | Oct-05 | Apr-06 | Apr-07 | Jun-07 | Nov-07 | Mar-08 | Sep-08 | Oct-08 |
| InSAR | 1.18 | 1.31 | 1.2 | 0.69 | 0.75 | 0.84 | 0.6 | 0.32 | 0.58 | 0.63 |
| MM5 | 0.74 | 0.76 | 0.9 | 0.54 | 0.35 | 0.58 | 0.8 | 0.45 | 0.41 | 1.1 |

***Table I.*** *InSAR and MM5 standard deviations (mm of IWV), Track 172.*

| | Oct-03 | Feb-04 | Aug-06 | Sep-06 | Jan-07 | Mar-07 | Dec-07 | May-08 | Aug-08 | Oct-08 |
|---|---|---|---|---|---|---|---|---|---|---|
| InSAR | 0.51 | 0.49 | 1.1 | 0.54 | 0.87 | 0.76 | 0.6 | 0.96 | 0.92 | 1.08 |
| MM5 | 0.43 | 0.6 | 1.3 | 0.44 | 0.97 | 0.28 | 0.5 | 1.34 | 0.95 | 0.84 |

***Table II.*** *InSAR and MM5 standard deviations (mm of IWV), Track 351.*

where $k_0$ is a nominal value and $\delta k_i$ takes into account the possible changes.
Thus, the APS of a generic image i referred to a common master M can be written as

$$\begin{aligned}\alpha_{i,M} &= \varepsilon_i + k_i q - (\varepsilon_M + k_M q) = \\ &= \varepsilon_i - \varepsilon_M + \delta k_i q - \delta k_M q\end{aligned} \quad (4)$$

By averaging the stack of available APS's, it is possible to estimate just a differential component of the delay of the master acquisition,

$$\bar{\alpha}_M = \varepsilon_M + \delta k_M q \quad (5)$$

Thus, in order to compare "absolute" IWV maps to "absolute" APS maps, also the "nominal" IWV trend with height (the one linked to $k_0$), common in all IWV maps, has to be estimated and removed.

## 3. EXPERIMENTAL ANALYSIS

MM5 maps have been generated in correspondence of SAR acquisitions. In each day, 24 images have been created with a temporal sampling of 1 hour. Depending

| Nov-02 | Dec-02 | Aug-03 | Dec-03 | Jan-04 | Apr-04 | May-04 | Aug-04 | Oct-04 | Jan-05 |
|---|---|---|---|---|---|---|---|---|---|
| -0.15 | 0.43 | 0.37 | 0.26 | 0.79 | -0.12 | 0.23 | 0.47 | 0.23 | 0.76 |
| Jul-05 | Aug-05 | Oct-05 | Apr-06 | Apr-07 | Jun-07 | Nov-07 | Mar-08 | Sep-08 | Oct-08 |
| 0.40 | 0.52 | 0.74 | -0.35 | 0.20 | 0.34 | 0.37 | -0.01 | 0.42 | 0.36 |

***Table III.*** *Correlation coefficients of the scatter plots of Figure 7 (MM5 vs InSAR in Track 172).*

| Oct-03 | Feb-04 | Aug-06 | Sep-06 | Jan-07 | Mar-07 | Dec-07 | May-08 | Aug-08 | Oct-08 |
|---|---|---|---|---|---|---|---|---|---|
| 0.46 | -0.11 | 0.50 | -0.26 | -0.27 | 0.20 | 0.15 | -0.21 | -0.21 | -0.03 |

***Table IV.*** *Correlation coefficients of the scatter plots of Figure 6 (MM5 vs InSAR in Track 351).*

| | Nov-02 | Dec-02 | Aug-03 | Dec-03 | Jan-04 | Apr-04 | May-04 | Aug-04 | Oct-04 | Jan-05 |
|---|---|---|---|---|---|---|---|---|---|---|
| before | 0.51 | 0.49 | 1.08 | 0.54 | 0.87 | 0.76 | 0.59 | 0.96 | 0.92 | 1.08 |
| after | 0.71 | 0.59 | 1.33 | 0.60 | 0.61 | 0.84 | 0.66 | 1.23 | 1.16 | 0.70 |
| | Jul-05 | Aug-05 | Oct-05 | Apr-06 | Apr-07 | Jun-07 | Nov-07 | Mar-08 | Sep-08 | Oct-08 |
| before | 1.18 | 1.31 | 1.17 | 0.69 | 0.75 | 0.84 | 0.57 | 0.32 | 0.58 | 0.63 |
| after | 1.11 | 1.12 | 0.79 | 1.02 | 0.76 | 0.84 | 0.82 | 0.55 | 0.55 | 1.05 |

***Table V.*** *InSAR IWV standard deviation [mm] before and after removal of the MM5 values. Track 172. In red: cases in which the IWV standard deviation decreases.*

| | Oct-03 | Feb-04 | Aug-06 | Sep-06 | Jan-07 | Mar-07 | Dec-07 | May-08 | Aug-08 | Oct-08 |
|---|---|---|---|---|---|---|---|---|---|---|
| before | 0.48 | 0.62 | 1.85 | 0.87 | 0.64 | 0.48 | 0.42 | 0.47 | 0.82 | 0.62 |
| after | 0.52 | 1.07 | 1.62 | 1.08 | 0.78 | 0.62 | 0.72 | 0.75 | 1.16 | 0.82 |

***Table VI.*** *InSAR IWV standard deviation [mm] before and after removal of the MM5 values. Track 351. In red: cases in which the IWV standard deviation decreases.*

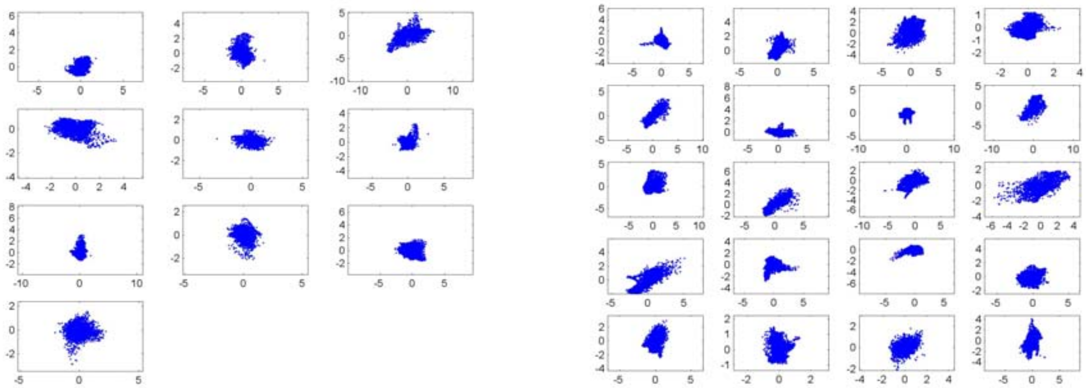

**Figure 3.** Scatter plot between InSAR (ordinate) and MM5 (abscissa) IWV in [mm]. Left descending, right ascending Envisat orbits over Rome.

on the SAR acquisition time (different form ascending and descending passes) the corresponding MM5 map has been used for the comparison.

The first analysis has been carried out exploiting an ERS1 dataset acquired during the 3 days phase in '94. 27 ERS1 images have been processed over Rome and 7 APS of the dataset have been compared with corresponding MM5 maps. Figure 1 shows a comparison example, reporting from left to right, starting from the first raw: 1a) MM5 map, 1b) InSAR APS, 1c) difference between InSAR and MM5, 1d) scatter plot between InSAR and MM5 values, 1e) histogram of the difference values, 1f) difference values as a function of the terrain height. All parameters are in mm of IWV. From Figure 1 it can be seen that the InSAR map has a higher variability than the MM5 one. (figs 1a and 1b) The two data anyway reproduce similar features that can be found related to the local topography and show a moderate correlation (fig 1d). Part of the unexplained residual APS (about 1.5 mm dispersion, fig 1e) is still correlated with the topography (fig 1f). In the few analyzed available data from the '94 dataset, about 50% of MM5 maps have shown to successfully mitigate InSAR APS, up to a reduction of 30% of the total APS power, most information being contained in the vertical stratification.

We conducted further analysis using Envisat acquisitions from 2002 to late 2008. Twenty MM5 maps have been generated at track 172 data takes, and ten maps during track 351 passes. Figure 2 reports the domain in which MM5 calculates the IWV values, with a resolution of 1km.

The strategy chosen for comparing InSAR and MM5 IWV maps is the one described in the previous section for which, after compensating for linear trends in each data, the average IWV images are calculated in the two datasets and removed from the data. Then, delay values are converted into mm of precipitable water vapor. The

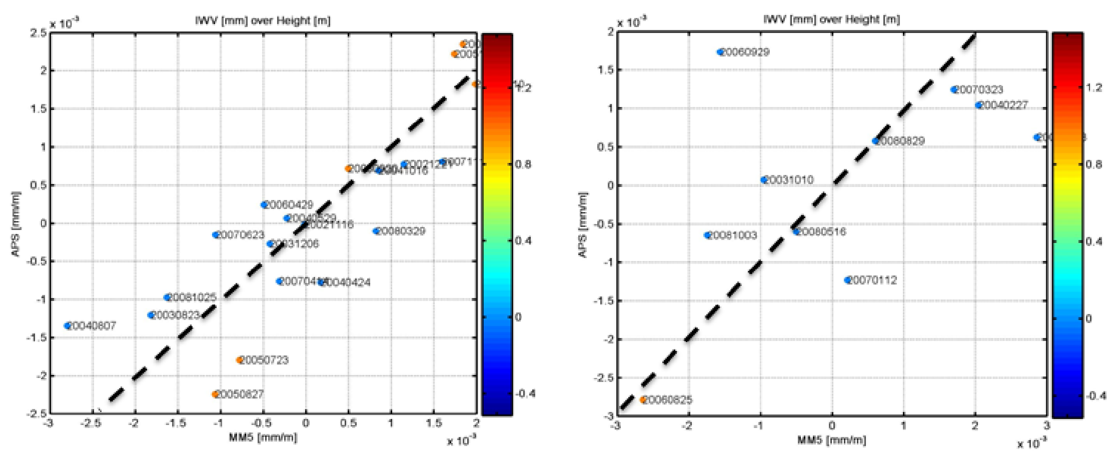


**Figure 4.** Scatter plot between InSAR (ordinate) and MM5 (abscissa) $\delta k_i$ in [mm/m]. Left desce, right asce Envisat orbits over Rome.

final data are plotted in Figure 3 for the two analyzed tracks. Unless otherwise indicated, in the following images and tables, the data are reported in chronological order row by row from left to right starting from the upper line.

Firstly, the differential IWV values retrieved by the two techniques have similar standard deviation, on average around 0.7mm (as shown in Table I and II). By looking more in detail, MM5 has slightly lower values than InSAR (0.61 vs 0.72 in the morning and 0.71 vs 0.79 in the evening). In second instance, we can notice in general a weak correlation, with some good cases (in particular in the ascending track) and some others in which the correlation is quite low (see Tables III and IV).

Next step is to roughly evaluate the global effect of mitigating the InSAR APS with MM5 maps. Tables V and VI show the InSAR IWV standard deviation variation before and after correcting for MM5 IWV data. Roughly, in 6 cases out of 20 for the ascending track and in 1 case out of 10 for the descending track, MM5 is able to reduce the power of the InSAR APS. In the other cases, we have some invariant situation but also considerable worsenings.

A more advanced analysis is able to add further insights to the problem at hand. As mentioned in the previous subsection, we investigate the relations between the turbulent and the stratification terms of IWV. In particular, Figure 4 reports the scatter plots between the IWV differential height trend ($\delta k_i$ in eq. (3)) estimated from InSAR and MM5. The result is particularly significant. Figure 4 on the right shows the outcome for the ascending track. From that plot a good correlation can be found between the differential height trend estimated in InSAR and the one retrieved with MM5 (scatter plot dispersion around 0.7 mm/km, against 1.3 mm/km InSAR dispersion). The two methodologies are basically measuring the same phenomenon, with a precision at the moment not yet found in other instruments. But Figure 4 shows also with color which are the data in which MM5 decreases the InSAR dispersion (marked with orange). As visible from the plot, those data group in the upper and lower parts, where the IWV stratification term is higher. When the height dependent term is higher than turbulence, MM5 is able to partially correct InSAR APS. But when the stratification term is low, MM5 cannot predict the turbulence.

Figure 4 on the left, reporting the same result for the descending track, shows a higher dispersion than in the ascending track, but the final outcome is pretty in accordance.

## 4. CONCLUSIONS

In this work we experimentally analyze the capability of the MM5 NWP model to mitigate the atmospheric artefacts that affect SAR interferograms. To this aim we processed data acquired over Rome by ERS1 in the 3 days phase in ’94 and by Envisat in recent years. Whilst archived data taken in ’94 match just in 50% of cases, the height-IWV linear trends estimated in Envisat data agrees well with MM5 ones. Unfortunately, the cases in which the topography-dependent APS term is stronger than the turbulent one are not predominant. Therefore, at the moment MM5 cannot be used yet as an operational tool for mitigating atmospheric delays. Further research and development are needed to improve non-SAR APS estimates.

## 5. REFERENCES


[1] Foster, J., Brooks, B., Cherubini, T., Shacat, C., Businger, S., Werner, C. L.: Mitigating atmospheric noise for InSAR using a high resolution weather model, Geophysical Research Letters, vol. 33, L16304, 2006.

[2] Webley, P.W., Bingley, R.M., Dodson, A.H., Wadge, G., Waugh, S.J., James, I.N.: Atmospheric water vapour correction to InSAR surface motion measurements on mountains: results from a dense GPS network on Mount Etna, Physics and Chemistry of the Earth 27, 363-370, 2002.

[3] Dudhia, J.: A nonhydrostatic version of the Penn State-NCAR Mesoscale Model: validation tests and simulation of an atlantic cyclone and cold front. Mon. Wea. Rev., 129, 1493-1513, 1993.

[4] Ferretti, A., Prati, C., Rocca, F.: Permanent Scatterers in SAR Interferometry, IEEE TGARS, Vol. 39, no. 1, 2001.

[5] Emardson, T.R., Derks, H.J.P., 2000. On the relation between wet delayand the integrated precipitable water vapour in the European atmosphere. Meteorological Applications 7, 61–68.

[6] Onn, F. 2007, “Modeling water vapor using GPS with application to mitigating InSAR atmospheric distortions”, PhD thesis, Stanford University, 2007.

[7] J. Saastamoinen, Contribution to the theory of atmospheric refraction. Bull. Géodésique 107 (1973), pp. 13–34.